Asymmetric Optical Transitions Determine the Onset of Carrier Multiplication in Lead Chalcogenide Quantum Confined and Bulk Crystals

Supporting Information

Frank C. M. Spoor,[†] Gianluca Grimaldi,[†] Christophe Delerue,[‡] Wiel H. Evers,[†] Ryan W. Crisp,[†] Pieter Geiregat,[§] Zeger Hens,[§] Arjan J. Houtepen[†] and Laurens D. A. Siebbeles*[†]*

[†]Chemical Engineering Department, Delft University of Technology, Van der Maasweg 9, 2629 HZ Delft, The Netherlands

[‡]IEMN, Département ISEN, UMR CNRS, 59046 Lille Cedex, France

[§]Physics and Chemistry of Nanostructures, Ghent University, 9000 Ghent, Belgium

Carrier multiplication measurements

The CM characteristics in our colloidal PbSe and PbS QDs were determined from TA spectroscopy measurements following a well-established method.[1-3] First the bleach at the band gap was measured for a broad range of photoexcitation energies and pump fluences. In Figure S1a we show a typical TA spectrum around the band edge bleach for 3.9 nm PbSe QDs photoexcited at 3.5 eV (350 nm) together with the ground-state absorption spectrum. At 5 ps pump-probe delay, all initially hot charge carriers have cooled down to the band edge. Multiple electron-hole pairs can however be present in a single QD due to CM or multi-photon absorption. Multi-photon absorption in colloidal QDs follows a Poisson distribution, with the probability P_N of absorbing N photons in one QD given by

$$P_N = \frac{e^{-\langle N \rangle}\langle N \rangle^N}{N!} \quad (1)$$

where $\langle N \rangle = J\sigma$ is the average number of photons absorbed per QD determined from the photon fluence J and the absorption cross section σ. If multiple electron-hole pairs are present in a QD, Auger decay takes place until only a single cold electron-hole pair is left. At 1 ns pump-probe delay all Auger decay has taken place, since the typical timescale of Auger decay in PbSe QDs is tens of picoseconds, while single electron-hole pairs have a lifetime of hundreds of nanoseconds.[4] In Figure S1b we show the evolution of the band edge bleach when no Auger decay is present and when Auger decay does occur.

The band edge bleach in PbSe QDs scales linearly with the number of electron-hole pairs present.[3] By dividing the band edge bleach at 5 ps pump-probe delay with the band edge bleach at 1 ns pump-probe delay the ratio of population R_{pop} is determined. R_{pop} equals the total number of electron-hole pairs created divided by the number of QDs that have been photoexcited in the ensemble. R_{pop} is therefore equal to

$$R_{\mathrm{pop}} = \frac{J\sigma \mathrm{QY}}{1-e^{-J\sigma}} \quad (2)$$

Here the quantum yield, QY, is the number of electron-hole pairs created per absorbed photon. The factor $e^{-J\sigma}$ in the denominator is the probability in the Poisson distribution of equation (1) that no photon is absorbed in a QD. The total denominator is therefore the fraction of QDs in the ensemble that have absorbed at least one photon. For low photon fluence and low photon energy where no CM occurs, R_{pop} is equal to one. Upon increasing the fluence, R_{pop} rises above one due to multi-photon absorption. When the photon energy is sufficiently high that CM does occur, R_{pop} is equal to the QY for low fluence and rises above this value when the fluence is increased.

In Figure S1c we show fits of equation (2) to R_{pop} as a function of pump photon fluence for various photon energies for 2.0 nm PbSe QDs. Indeed R_{pop} is constant at low fluence for each photon energy and rises when the fluence is increased. Fitting equation (2) to the data yields the QY, shown in Figure S1d as a function of photon energy normalized by the band gap energy for 2.0 nm PbSe QDs. As expected the QY is always one for photon energies below twice the band gap energy, since energy conservation prevents CM. We determine the CM threshold, E_{th}, and the CM efficiency, η, from a linear fit to the QY data exceeding one. The normalized photon energy at which this fit gives a QY of one is defined as the CM threshold.[5-7] The slope of the line is the CM efficiency, the number of electron-hole pairs produced per unit normalized photon energy above the threshold. In the main text we discuss that although a linear fit is useful to facilitate discussion of CM, the QY does not necessarily increase linearly with photon energy. The QY for all our colloidal PbSe and PbS QDs was determined according to the above described procedure.

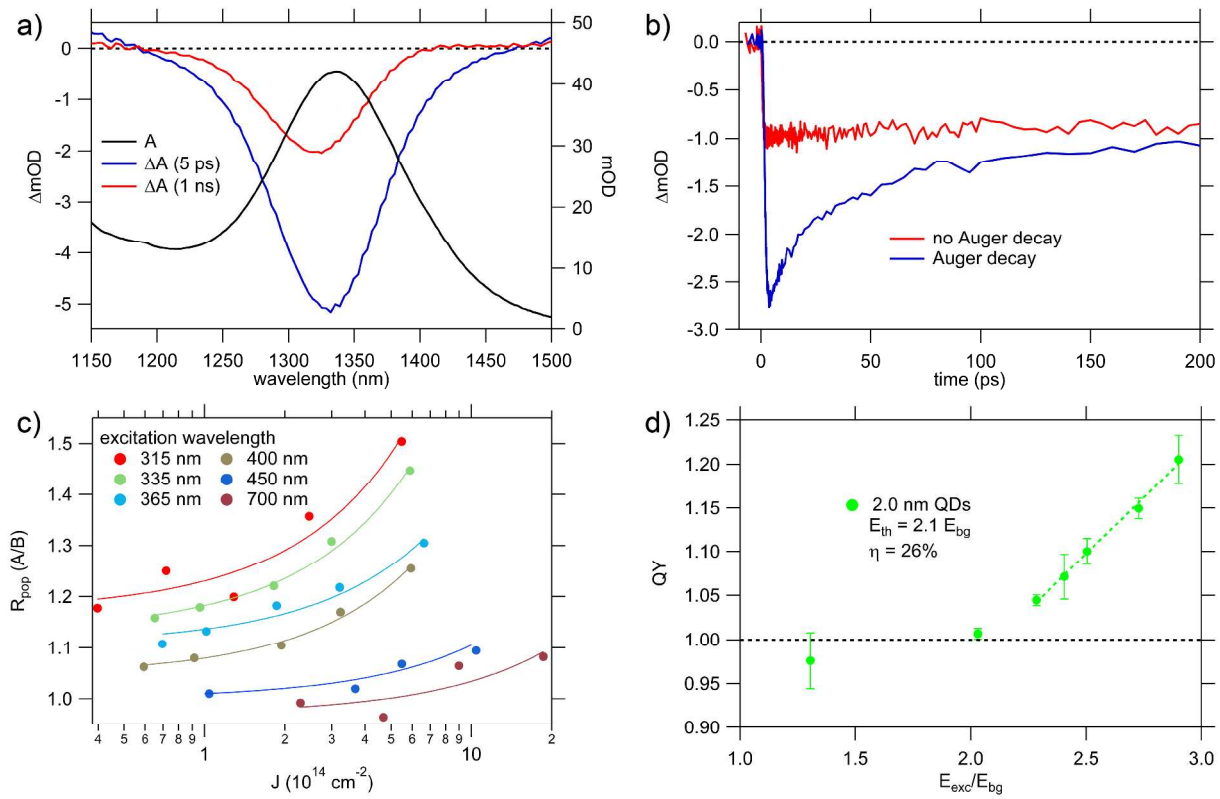

Figure S1. a) TA spectrum around the band edge bleach (left axis) for 3.9 nm PbSe QDs photoexcited at 3.5 eV (350 nm), together with the ground-state absorption spectrum A (right axis). b) Evolution of the band edge bleach for 3.9 nm PbSe QDs with and without Auger decay. c) R_{pop} as a function of pump photon fluence for various photon energies for 2.0 nm PbSe QDs, including fits of equation (2). d) QY as a function of photon energy normalized by the band gap energy for 2.0 nm PbSe QDs. The linear fit is used to determine the CM threshold and CM efficiency.

Carrier multiplication results

Following the above described procedure, we have measured the QY in 6 sizes of PbSe QDs and 5 sizes of PbS QDs. The QY as a function of photon energy normalized by the band gap energy for all QDs ordered from small to large is shown in Figure S2 for PbSe and in Figure S3 for PbS. For every size the CM threshold E_{th} and the CM efficiency η are determined from a linear fit to the QY data exceeding unity. It can be observed that for both materials, the CM threshold is lowest for the smallest QDs and increases with QD size. The CM efficiency follows the same trend. It was suggested that the CM threshold and CM efficiency are coupled in the model of Beard *et al.*[8, 9] This model is however invalid when higher bands are involved that can influence both cooling and the II rate. We do not observe the same trend and consider the CM threshold and CM efficiency as independent variables.

From Figure S2 and Figure S3 we observe that the CM threshold coincides with the $L_{4\text{-}6}$ and $L_{5\text{-}7}$ transition energies.[10] These transition energies are less dependent on quantum confinement than the band gap energy and therefore become smaller on a normalized photon energy scale as the QDs are reduced in size. For the smallest PbSe QD of 1.3 nm, the $L_{4\text{-}6}$ and $L_{5\text{-}7}$ transition energies are smaller than two times the band gap energy. Interestingly, scanning the photoexcitation energy up to 4 eV or 2.5 times the band gap energy, we were unable to observe any CM in this sample. We would expect a lower CM threshold than 2.5, since the CM threshold increases with QD size and larger PbSe QDs have a lower CM threshold. This greatly strengthens the relation of the CM threshold to the $L_{4\text{-}6}$ and $L_{5\text{-}7}$ transitions, as discussed in the main text.

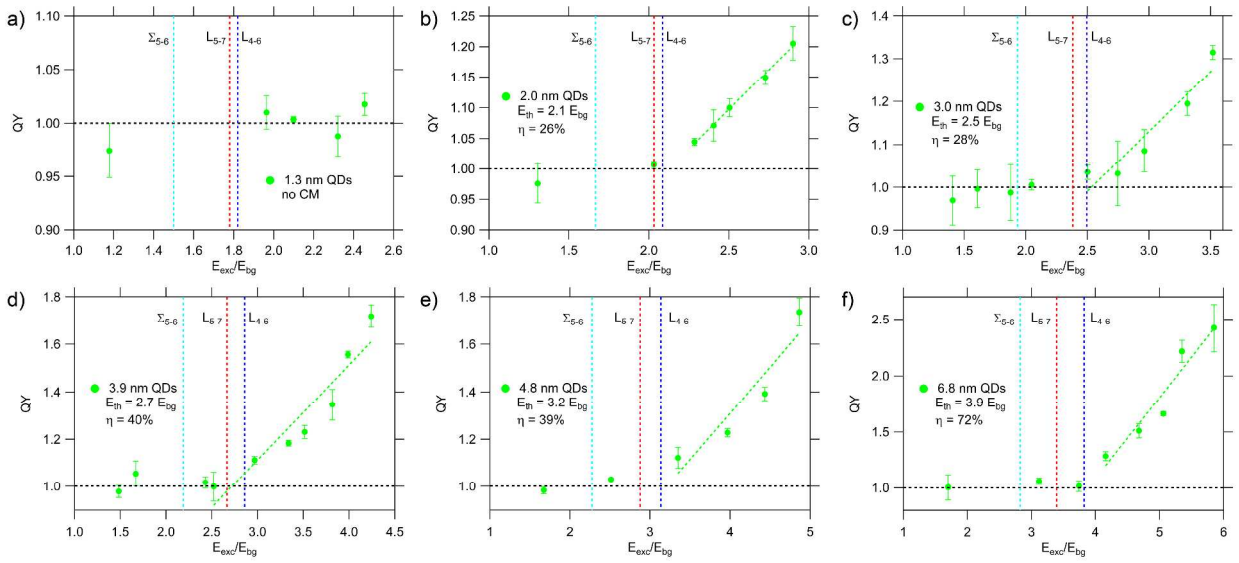

Figure S2. QY as a function of photon energy normalized by the band gap energy for PbSe QDs of size a) 1.3 nm, b) 2.0 nm, c) 3.0 nm, d) 3.9 nm, e) 4.8 nm and f) 6.8 nm. The linear fit is used to determine the CM threshold E_{th} and CM efficiency η. The Σ_{5-6}, L_{4-6} and L_{5-7} transition energies are included for comparison with the CM threshold.

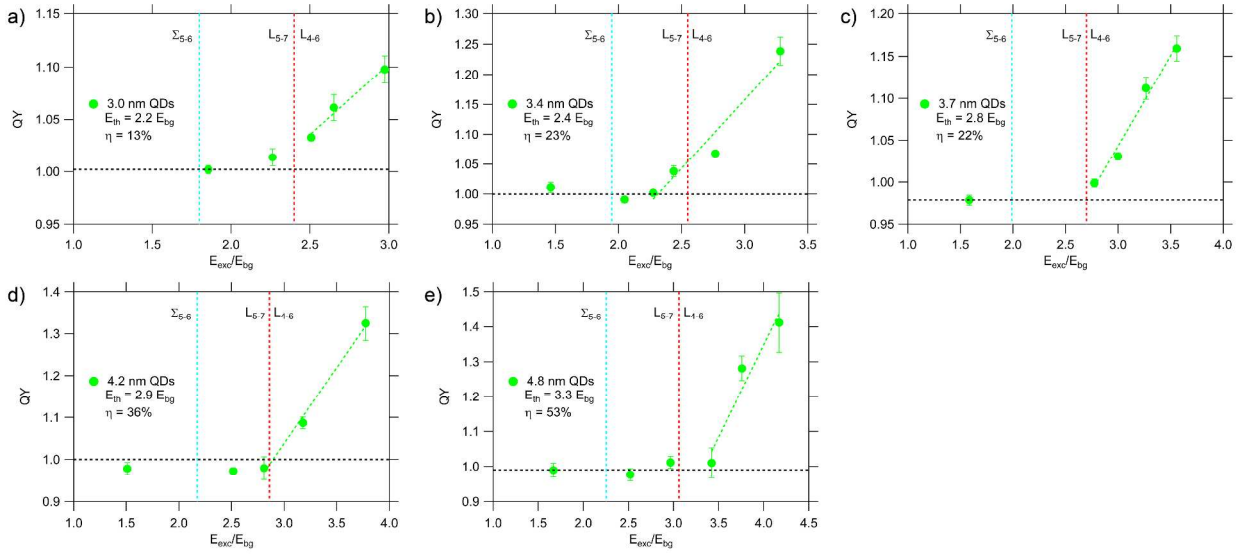

Figure S3. QY as a function of photon energy normalized by the band gap energy for PbS QDs of size a) 3.0 nm, b) 3.4 nm, c) 3.7 nm, d) 4.2 nm and e) 4.8 nm. The linear fit is used to determine the CM threshold E_{th} and CM efficiency η. The Σ_{5-6}, L_{4-6} and L_{5-7} transition energies are included for comparison with the CM threshold.

Carrier multiplication as a function of absolute photon energy

As a comparison to the QY as a function of photon energy normalized by the band gap energy in Figure 2 of the main text, the QY for all PbSe and PbS QDs as a function of absolute photon energy is shown in Figure S4a and S4b. We observe that the CM threshold is highest for the smallest QDs and decreases with QD size. This is contrary to the increase of the CM threshold with QD size on a normalized photon energy scale. The CM efficiency still increases with QD size as before. The QY is higher for the larger QDs on an absolute photon energy scale as can observed in Figure S4a and Sb. This means that at any photon energy, more electron-hole pairs are created by CM in larger QDs than in smaller QDs. When CM is considered in applications such as solar cells however, the energy of the electron-hole pairs is also relevant. Although in the largest QDs more electron-hole pairs are created, their energy is lower than in smaller QDs due to the smaller band gap. When the photon energy is normalized by the band gap energy as in Figure 2 of the main text, the energy of the created electron-hole pairs is taken into account. The CM threshold is then lowest for the smallest QDs. This means that the extra energy that can be harvested through CM is higher in smaller QDs than in larger QDs. These observations agree with the argument of Beard *et al.*.[8]

We also compare the absolute $\Sigma_{5\text{-}6}$, $L_{4\text{-}6}$ and $L_{5\text{-}7}$ transitions energies to the CM threshold as a function of band gap energy in Figure S4c and S4d for PbSe and PbS QDs and bulk.[10-12] We observe that the CM threshold still coincides with the occurrence of the $L_{4\text{-}6}$ and $L_{5\text{-}7}$ transitions on an absolute photon energy scale. The transition energies drop below the energy conservation limit for CM of twice the band gap energy, indicated by the black dashed line, if the QDs are too small. Hence, the nature of the optical transition determines the CM threshold in both PbSe and PbS QDs and bulk, while the energies of the band gap and of the asymmetric transitions depend on the extent of quantum confinement.

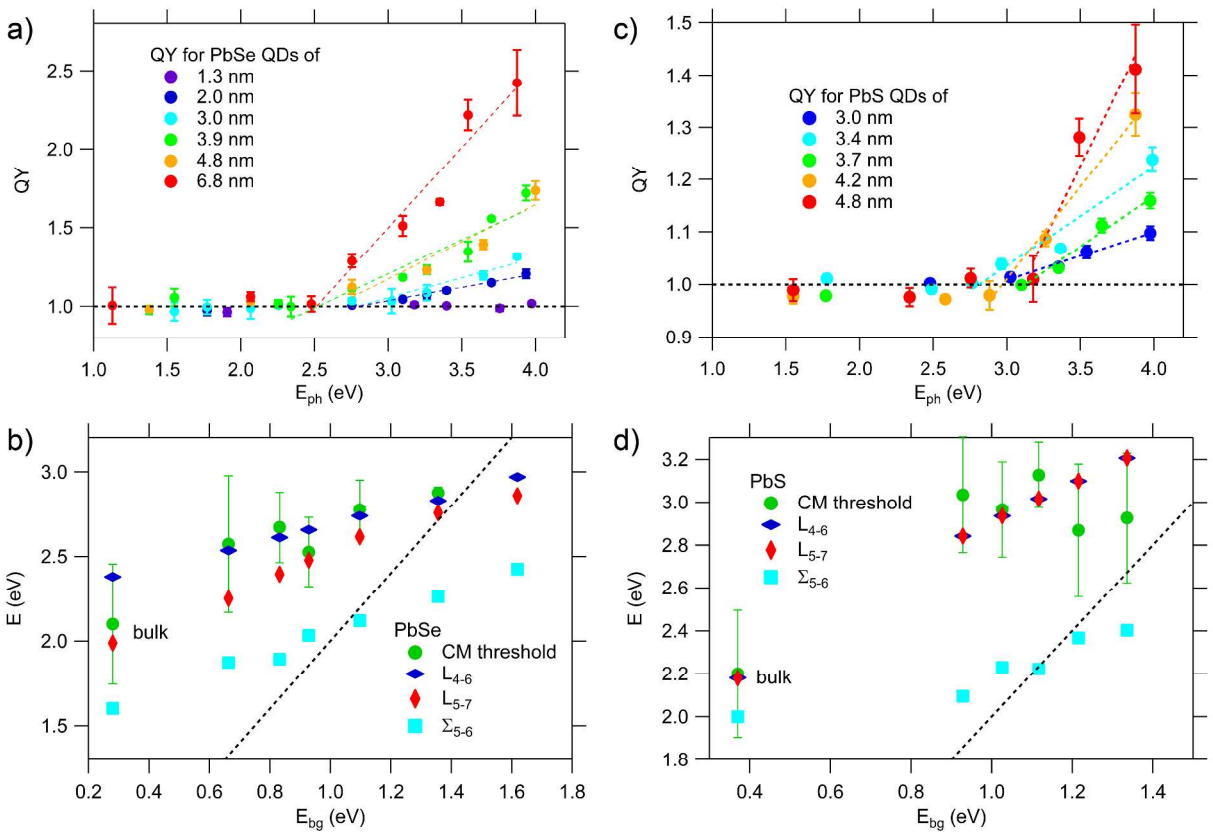

Figure S4. a) and b) QY as a function of absolute photon energy for various sizes of PbSe and PbS QDs. c) and d) Absolute $\Sigma_{5\text{-}6}$, $L_{4\text{-}6}$ and $L_{5\text{-}7}$ transition energies and the CM threshold as a function of band gap energy for PbSe and PbS QDs and bulk. The black dashed line indicates the energy conservation limit for CM. Bulk data was taken from the work of Pijpers *et al.*[11]

Cooling and impact ionization rate

In our previous work we reported a broadband cooling spectrum of electrons and holes as a function of photon energy for 3.9 nm PbSe QDs.[13] At photon energies relevant for CM, starting at twice the band gap energy, we found a continuously increasing cooling time for electrons from which we extracted an energy loss rate γ. For 3.9 nm PbSe QDs with a band gap of 0.95 eV, we find an energy loss rate γ = 1-5 eV/ps at high photon energy. From this energy loss rate and data of the QY for 3.9 nm PbSe QDs from Figure S2d, we can estimate an experimental II rate at the CM threshold.

As stated in our previous work, cooling at high excess energy is likely governed by LO phonon emission.[13] We therefore propose to use an electronic structure such as shown in Figure S5a, representing a ladder of N equidistant energy levels. The lowest level is at the CM energy conservation limit of one band gap energy above the band edge (1.9 eV), the highest level at the energy at which a hot electron is initially created.

Now we consider how a hot electron cools down through the electronic structure of Figure S5a. We assume that in each energy level, an electron has the possibility of either undergoing II or cooling down to the highest energy level below as shown in Figure S5b. For simplicity we assume that the cooling rate k_{cool} and the II rate k_{II} are the same in each energy level and that an electron can only undergo II once. A hot electron in this model can therefore have a maximum excess energy of twice the band gap energy. We define ΔE as the hot electron energy above the CM energy conservation limit and δE as the energy distance between successive energy levels, see Figure S5a. Assuming that cooling is only governed by LO phonon emission the energy loss rate is given by

$$\gamma \approx \delta E k_{\mathrm{cool}} \tag{3}$$

so that k_{cool} becomes

$$k_{\text{cool}} = \frac{\gamma}{\delta E} = N\frac{\gamma}{\Delta E} \quad (4)$$

The cooling rate in equation (4) is linearly dependent on the number of energy levels *N*. Defining a fixed energy loss rate from experiments, we will show that for a number of energy levels *N* high enough, the II rate is independent of *N*.

The probability of cooling down an energy level instead of undergoing II (both processes shown in Figure S5b) is given by the ratio of the rates of these processes according to

$$p_{\text{cool}} = \frac{k_{\text{cool}}}{k_{\text{cool}}+k_{\text{II}}} \quad (5)$$

The probability that an electron does not undergo II and therefore relaxes *via N* cooling steps to below the CM energy conservation limit is equal to $(p_{\text{cool}})^N$. The total probability of an electron undergoing II in any of the energy levels is therefore $1-(p_{\text{cool}})^N$. This probability is equal to the QY – 1. Using this and equation (5), the QY becomes

$$\text{QY} = 1 - \left(\frac{k_{\text{cool}}}{k_{\text{cool}}+k_{\text{II}}}\right)^N + 1 \quad (6)$$

Equation (6) can now be used to estimate the II rate from the QY and the energy loss rate, which is converted to k_{cool} using equation (4). Note that under the assumption that cooling is only governed by LO phonon emission, equation (6) is only usable near the CM threshold where cooling by II is still negligible.

To arrive at an experimental estimate of the II rate for 3.9 nm PbSe QDs, we use the first QY data point exceeding unity in Figure S2d. For this data point, the QY = 1.1 at a normalized photon energy of 2.95 times the band gap energy. This is equivalent to a photon excess energy over the CM energy conservation limit of 0.9 eV. Although the excess photon energy may be divided between the electron and hole, we assume an electron excess energy of ΔE = 0.9 eV to provide a lower bound to the estimated II rate. We use an energy loss rate of γ = 2.5 eV/ps for 2.95 times the band gap energy from our previous work.[13] When cooling is governed by LO

phonon emission, the distance between energy levels can be set equal to the LO phonon energy in PbSe of 17 meV.[14] Although many more energy levels exist and cooling by lower energy TA or LA phonons is possible, a minimum of N energy levels 17 meV apart is reasonable. Using the parameters $\gamma = 2.5$ eV/ps and $\Delta E = 0.9$ eV, equation (4) yields a cooling rate of $k_{cool} = 147$ ps^{-1} with $N = 53$ for $\delta E = 17$ meV.

In Figure S5c we show the QY as a function of k_{II}, calculated using equation (6), for $\gamma = 2.5$ eV/ps, $\Delta E = 0.9$ eV and various numbers of energy levels N. The QY = 1.1 is indicated by the black dashed line. We observe that equation (6) converges for large N. Any number of energy levels $N > 10$ yields comparable results for the QY. The value of $N = 53$ for the parameters mentioned above is clearly large enough. We find a lower bound to the II rate of $k_{II} \geq 0.3$ ps^{-1}. This experimental estimate of $k_{II} = 0.3$ ps^{-1} is equal to the II rate estimated in the main text when comparing the cooling data to tight-binding theory.

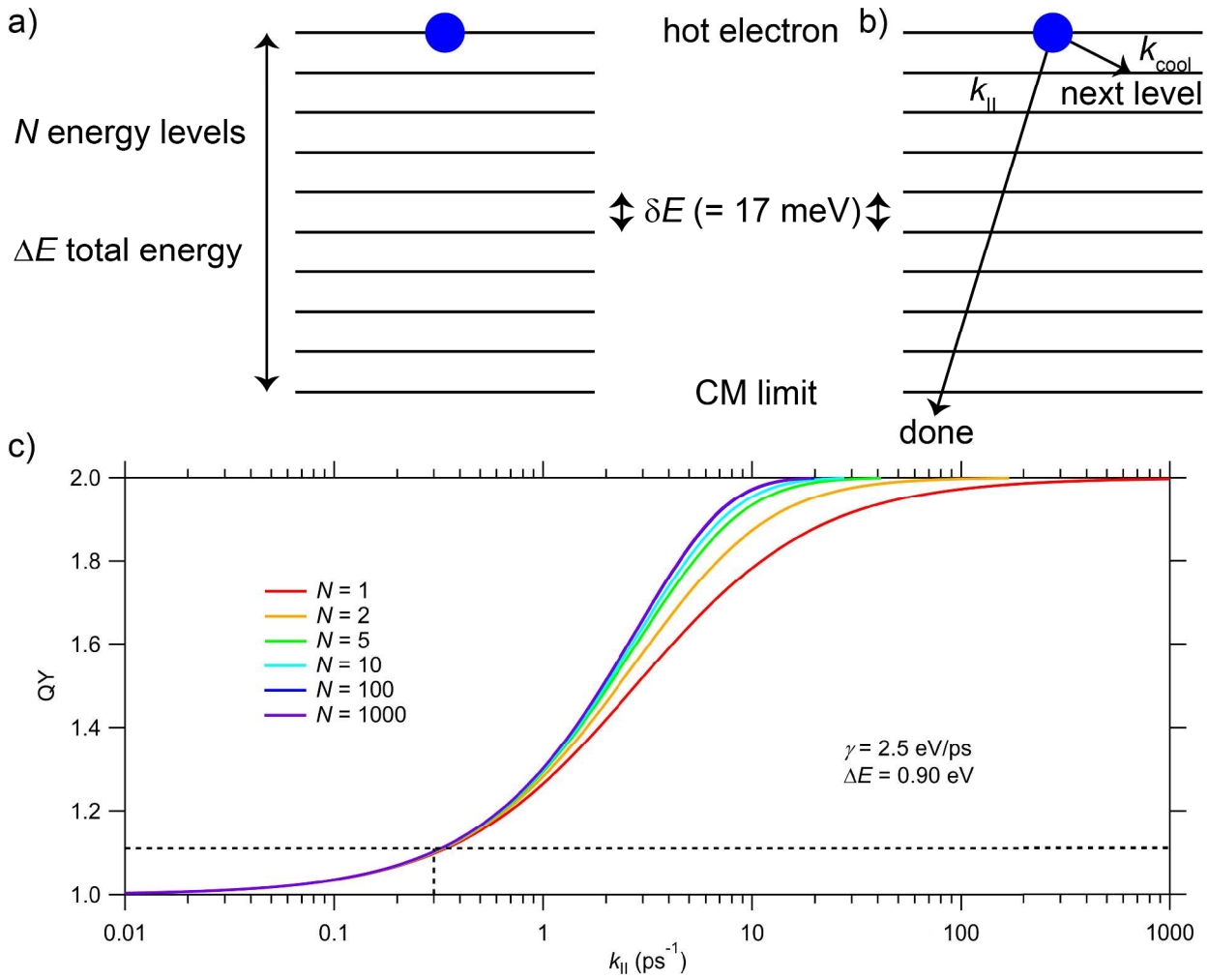

Figure S5. a) PbSe QD electronic structure with a ladder of N equidistant energy levels, starting at the CM energy conservation limit of twice the band gap energy, up to ΔE electron excess energy above it. b) The possibilities of II and cooling indicated in the PbSe QD electronic structure. c) QY as a function of k_{II}, calculated using equation (6), for $\gamma = 2.5$ eV/ps, $\Delta E = 0.9$ eV and various numbers of energy levels N. The QY = 1.1 is indicated by the black dashed line.

References

1. Schaller, R. D.; Klimov, V. I. High Efficiency Carrier Multiplication in PbSe Nanocrystals: Implications for Solar Energy Conversion. *Phys. Rev. Lett.* **2004,** 92, 186601.

2. Ellingson, R. J.; Beard, M. C.; Johnson, J. C.; Yu, P.; Micic, O. I.; Nozik, A. J.; Shabaev, A.; Efros, A. L. Highly Efficient Multiple Exciton Generation in Colloidal PbSe and PbS Quantum Dots. *Nano Lett.* **2005,** 5, 865-871.

3. Trinh, M. T.; Houtepen, A. J.; Schins, J. M.; Hanrath, T.; Piris, J.; Knulst, W.; Goossens, A. P. L. M.; Siebbeles, L. D. A. In Spite of Recent Doubts Carrier Multiplication Does Occur in PbSe Nanocrystals. *Nano Lett.* **2008,** 8, 1713-1718.

4. Wehrenberg, B. L.; Wang, C.; Guyot-Sionnest, P. Interband and Intraband Optical Studies of PbSe Colloidal Quantum Dots. *J. Phys. Chem. B* **2002,** 106, 10634-10640.

5. Aerts, M.; Suchand Sandeep, C. S.; Gao, Y.; Savenije, T. J.; Schins, J. M.; Houtepen, A. J.; Kinge, S.; Siebbeles, L. D. A. Free Charges Produced by Carrier Multiplication in Strongly Coupled PbSe Quantum Dot Films. *Nano Lett.* **2011,** 11, 4485-4489.

6. Sandeep, C. S. S.; Cate, S. t.; Schins, J. M.; Savenije, T. J.; Liu, Y.; Law, M.; Kinge, S.; Houtepen, A. J.; Siebbeles, L. D. A. High Charge-Carrier Mobility Enables Exploration of Carrier Multiplication in Quantum-Dot Films. *Nat. Commun.* **2013,** 4, 2360.

7. Aerts, M.; Bielewicz, T.; Klinke, C.; Grozema, F. C.; Houtepen, A. J.; Schins, J. M.; Siebbeles, L. D. A. Highly Efficient Carrier Multiplication in PbS Nanosheets. *Nat. Commun.* **2014,** 5, 3789.

8. Beard, M. C.; Midgett, A. G.; Hanna, M. C.; Luther, J. M.; Hughes, B. K.; Nozik, A. J. Comparing Multiple Exciton Generation in Quantum Dots To Impact Ionization in Bulk Semiconductors: Implications for Enhancement of Solar Energy Conversion. *Nano Lett.* **2010,** 10, 3019-3027.

9. Midgett, A. G.; Luther, J. M.; Stewart, J. T.; Smith, D. K.; Padilha, L. A.; Klimov, V. I.; Nozik, A. J.; Beard, M. C. Size and Composition Dependent Multiple Exciton Generation Efficiency in PbS, PbSe, and PbSxSe1–x Alloyed Quantum Dots. *Nano Lett.* **2013,** 13, 3078-3085.

10. Spoor, F. C. M.; Kunneman, L. T.; Evers, W. H.; Renaud, N.; Grozema, F. C.; Houtepen, A. J.; Siebbeles, L. D. A. Hole Cooling Is Much Faster than Electron Cooling in PbSe Quantum Dots. *ACS Nano* **2016,** 10, 695-703.

11. Pijpers, J. J. H.; Ulbricht, R.; Tielrooij, K. J.; Osherov, A.; Golan, Y.; Delerue, C.; Allan, G.; Bonn, M. Assessment of Carrier-Multiplication Efficiency in Bulk PbSe and PbS. *Nat. Phys.* **2009,** 5, 811-814.

12. Geiregat, P.; Delerue, C.; Justo, Y.; Aerts, M.; Spoor, F. C. M.; Van Thourhout, D.; Siebbeles, L. D. A.; Allan, G.; Houtepen, A. J.; Hens, Z. A Phonon Scattering Bottleneck for Carrier Cooling in Lead Chalcogenide Nanocrystals. *ACS Nano* **2015,** 9, 778-788.

13. Spoor, F. C. M.; Tomić, S.; Houtepen, A. J.; Siebbeles, L. D. A. Broadband Cooling Spectra of Hot Electrons and Holes in PbSe Quantum Dots. *ACS Nano* **2017,** 11, 6286-6294.

14. Habinshuti, J.; Kilian, O.; Cristini-Robbe, O.; Sashchiuk, A.; Addad, A.; Turrell, S.; Lifshitz, E.; Grandidier, B.; Wirtz, L. Anomalous Quantum Confinement of the Longitudinal Optical Phonon Mode in PbSe Quantum Dots. *Phys. Rev. B* **2013,** 88, 115313.